

WAVE-MEASUREMENT CAPABILITIES OF THE SURFACE CONTOUR RADAR AND THE AIRBORNE OCEANOGRAPHIC LIDAR

The 36-gigahertz surface contour radar and the airborne oceanographic lidar were used in the SIR-B underflight mission off the coast of Chile in October 1984. The two systems and some of their wave-measurement capabilities are described. The surface contour radar can determine the directional wave spectrum and eliminate the 180-degree ambiguity in wave propagation direction that is inherent in some other techniques such as stereophotography and the radar ocean wave spectrometer. The Airborne Oceanographic Lidar can acquire profile data on the waves and produce a spectrum that is close to the nondirectional ocean-wave spectrum for ground tracks parallel to the wave propagation direction.

SURFACE CONTOUR RADAR

The surface contour radar (SCR) is a 36-gigahertz computer-controlled airborne radar¹ that generates a false-color-coded elevation map of the sea surface below the aircraft in real time. It can routinely produce ocean directional wave spectra with postflight data processing that have much higher angular resolution than pitch-and-roll buoys. The high spatial resolution and rapid mapping capability over extensive areas make the SCR ideal for studying fetch-limited wave spectra, diffraction and refraction wave patterns in coastal areas, and wave phenomena associated with hurricanes and other highly mobile events. The SCR is also being applied in areas other than producing directional wave spectra such as determining the scattering characteristics of waves and the topography and backscatter characteristics of ice. In measurement concept, the SCR is one of the most straightforward remote sensing instruments. It provides great ease of data interpretation since it involves a direct range measurement.

The SCR normally operates at an altitude of 400 to 800 meters. Figure 1 shows the nominal measurement geometry and the horizontal resolutions in terms of the aircraft altitude, h . An oscillating mirror scans a 1.4-degree half-power-width pencil beam laterally to measure the elevations at 51 evenly spaced points on the

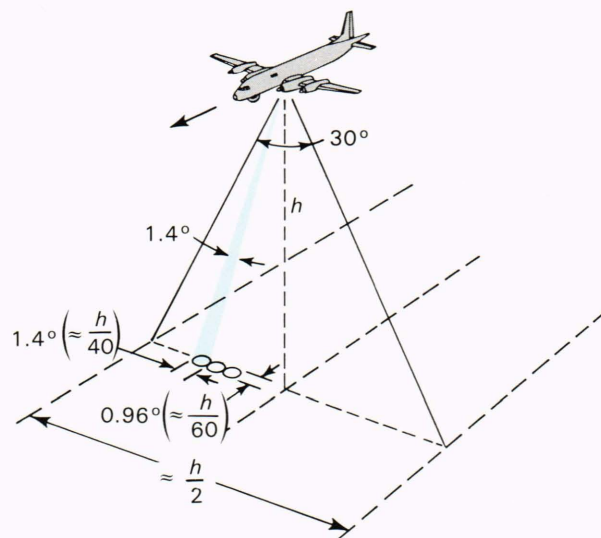


Figure 1—The basic measurement geometry and spatial resolution of the SCR.

surface below the aircraft. The nonscanning receiving antenna is a 1.3- × 40-degree fan beam with the 40-degree dimension oriented cross track. The combination of the transmit and receive antennas narrows the along-track interrogated region to a half-power width of 0.96 degree. At each of the 51 points across the swath, the SCR measures the slant range to the surface and corrects in real time for the off-nadir angle of the beam to produce the elevation of the point in question with respect to the horizontal reference.

The elevation measurements are false-color-coded and displayed on the SCR color TV monitor so that real-time estimates of significant wave height, dominant wavelength, and direction of propagation can be made.



Edward J. Walsh is an aerospace technologist at the NASA/Goddard Space Flight Center, Greenbelt, MD 20771. David W. Hancock and Donald E. Hines are with NASA/Goddard, Wallops Island, VA 23337. Robert N. Swift and John F. Scott are with EG&G

Washington Analytical Services Center, Pocomoke City, MD 21851.

The real-time display allows the optimal selection of aircraft altitude and flight-line direction even during a flight over a cloud-covered sea, without prior knowledge of the wave conditions. The radar has range resolution cells of 0.15, 0.3, 0.6, and 1.5 meters, although the last two cells have never been used for oceanographic studies. The 15-centimeter resolution has generally been used, with the 30-centimeter resolution employed when the significant wave height reaches 5 meters or when the SCR is operating at an altitude of 800 meters.

AIRBORNE OCEANOGRAPHIC LIDAR

The airborne oceanographic lidar (AOL), described by Hoge et al.,² was developed in the late 1970s by NASA in cooperation with several other federal agencies for the purpose of investigating and developing potential remote-sensing applications that can benefit from lidar technology performed from a high-speed, fixed-wing aircraft. The system uses one or more pulsed laser transmitters optically aligned with a receiving telescope and electro-optical components. The sensor can resolve, temporally and spectrally, backscattered laser or laser-stimulated fluorescence emission from ground or ocean targets, including bathymetry. In either mode, the AOL measures the range between the aircraft and the surface of the ground or ocean. After aircraft vertical motion is removed through postflight processing of the ranging data with measurements obtained from a vertical accelerometer, the system provides a high-precision measurement of the topographic features of the surface under investigation.

The laser system can profile the waves at a 400-hertz rate to provide independent corroboration of the elevation data measured by the SCR at the center of its swath. Figure 2 shows comparative data taken at an altitude of 230 meters by the SCR and AOL flying perpendicular to the crests of the waves. The data were obtained in the North Atlantic and the aircraft was traveling about 90 meters per second. The AOL data have been averaged to correspond to the SCR spot size in the along-track direction. The agreement is remarkable, considering that one system is microwave and the other is optical, that they use entirely different ranging techniques, and that the AOL is located 10 meters aft of the SCR in the aircraft and was looking aft at 15 degrees off-nadir. A relative shift in the time origin of approximately

0.7 second was required for the comparison of profiles between the two instruments. The 15-centimeter range quantization of the SCR is apparent in Fig. 2.

If the AOL profile data are Fourier transformed and Doppler corrected, the resulting spectrum is quite close to the nondirectional ocean spectrum for aircraft ground tracks that are parallel to the direction of propagation of the waves. The AOL proved quite useful in this regard on one of the Shuttle Imaging Radar (SIR-B) underflights during which neither the SCR nor the radar ocean wave spectrometer was operational.

COMPARISON OF SCR WITH PITCH-AND-ROLL BUOYS

Walsh et al.³ describe in detail the data processing used to produce directional wave spectra. They established the credibility of the SCR in the oceanographic community and demonstrated the limitations of pitch-and-roll buoys. Figures 3, 4, and 5 demonstrate the remarkable consistency of the Fourier coefficients of the directional-wave spectrum determined by the SCR compared to those of a variety of pitch-and-roll buoys. The model generally assumed in the oceanographic community for the spreading function (the azimuthal variation of the wave energy^{4,6}) is

$$A(s) \cos^{2s}((\theta - \theta_1)/2), \quad (1)$$

where $A(s)$ is a normalizing constant, θ_1 is the mean direction, and s is not necessarily an integer. If the spreading function is of the form given in Eq. 1, then there is a fixed relationship that must exist between r_1 and r_2 , which are the magnitudes of the fundamental and second harmonics of the Fourier coefficients of the spreading function.

Cartwright⁵ uses this theoretical relationship to test the consistency of the coefficients obtained from the National Institute of Oceanography pitch-and-roll buoy. His coefficients are shown at the top of Fig. 3, along with the theoretical relationship indicated by the solid curve. It is seen that the curve and the data follow the same trend, but almost all the data points lie to the left of the curve. Cartwright suggests that the discrepancies might be due to a bimodality of wind-wave spectra suggested by some results discussed by Longuet-Higgins et al.⁴ but considers it too complicated to treat in his

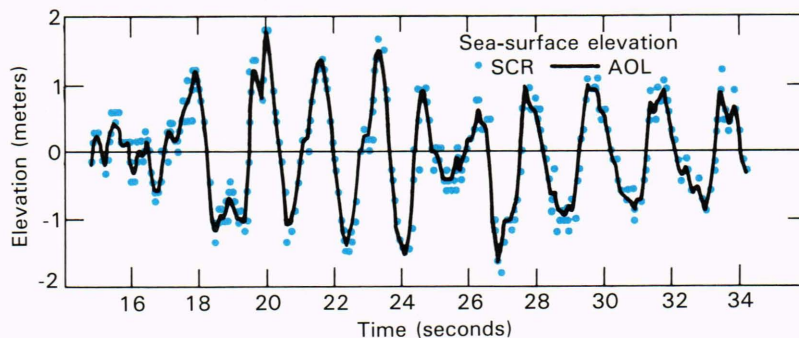


Figure 2—Comparison of wave profiles obtained simultaneously by the SCR and AOL at an altitude of 230 meters, flying perpendicular to the crests of the waves.

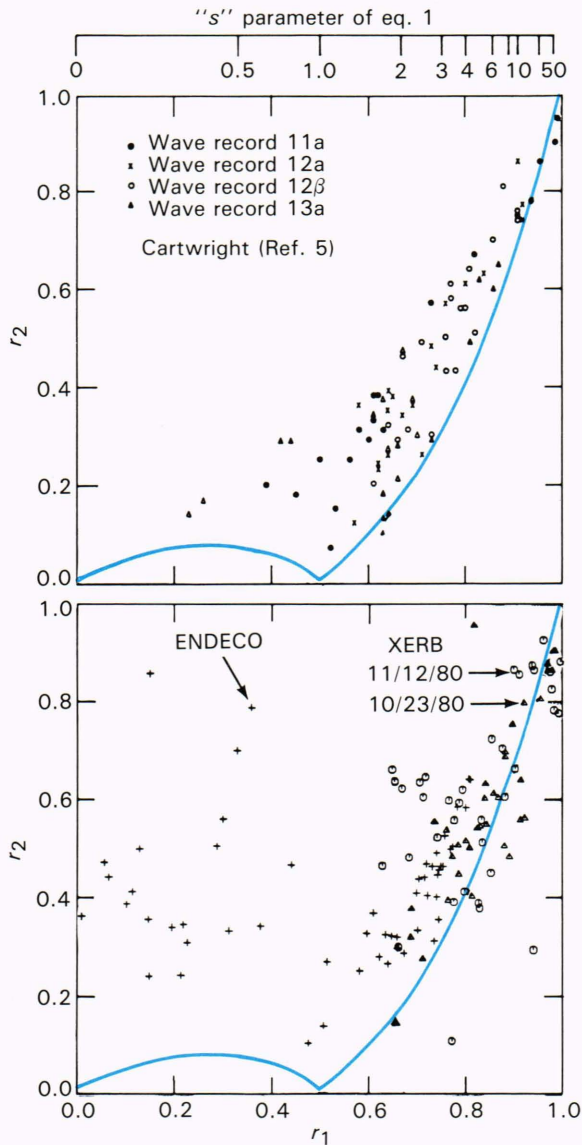


Figure 3—Amplitude ratios of the Fourier coefficients for data sets from the National Institute of Oceanography pitch-and-roll buoy (top of figure), and for the ENDECO and XERB pitch-and-roll buoys from ARSLOE data sets (bottom of figure), along with the curve indicating the theoretical ratio for a wave field satisfying Eq. 1.

analysis. The bottom of the figure shows the data points from the XERB and ENDECO pitch-and-roll buoys for the 1980 Atlantic Remote Sensing Land Ocean Experiment (ARSLOE).⁷ The ENDECO data points occupy the same position relative to the theoretical curve as the Cartwright data points, although ENDECO certainly has many outliers. The XERB data points lie on both sides of the curve, but the mean is still biased to the left. It should be pointed out that fewer points are plotted for XERB than for ENDECO because any points for which either r_1 or r_2 exceeded unity were not plotted since they were not physically realizable.

Figure 4 shows all the SCR data points from the three flights made during ARSLOE for the 400-meter (top)

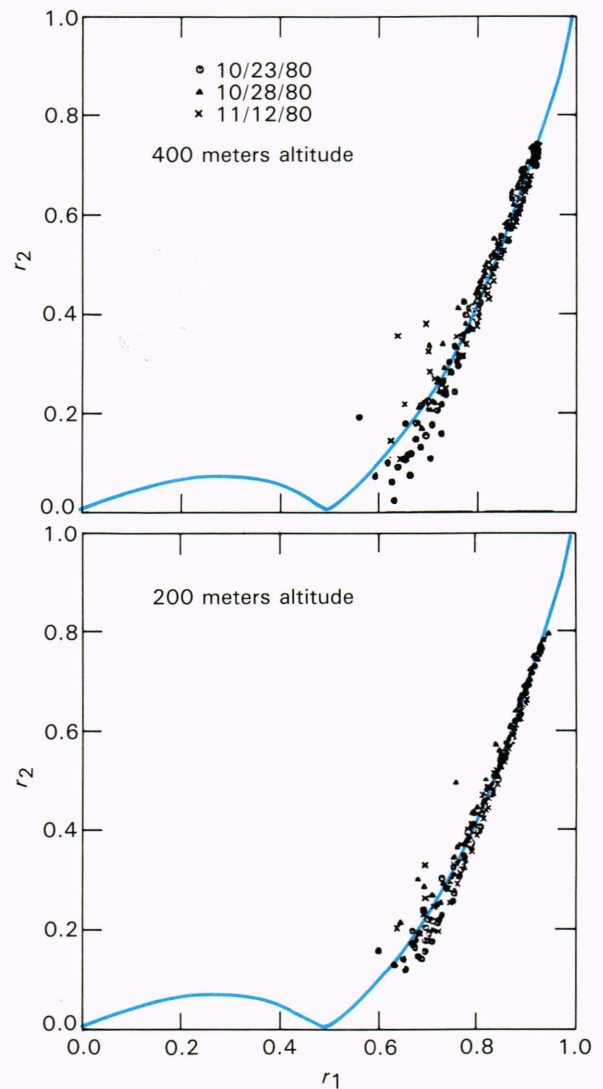


Figure 4—Amplitude ratios of the Fourier coefficients for the SCR ARSLOE data sets and the curve indicating the theoretical ratio for a wave field satisfying Eq. 1.

and 200-meter (bottom) altitudes. The time of the flights corresponded to the XERB and ENDECO data sets shown at the bottom of Fig. 3. Although different symbols are used for each day, the same symbol is used for the three ground tracks on a given day because analysis of the data showed no variation in the r_1 versus r_2 characteristic for the various ground tracks. Compared to the in-situ data of Fig. 3, the SCR data are an almost perfect fit to the theoretical curve.

In 1973, an extensive set of observations of the directional wave spectrum was made using the University of Hamburg meteorological buoy and an Institute of Ocean Sciences pitch-and-roll buoy during the Joint North Sea Wave Project (JONSWAP). Hasselmann et al.⁶ indicate that well-defined steady meteorological conditions were never encountered during the 20-day period of their study. However, they were able to select a number of cases under fairly steady wind conditions in the absence

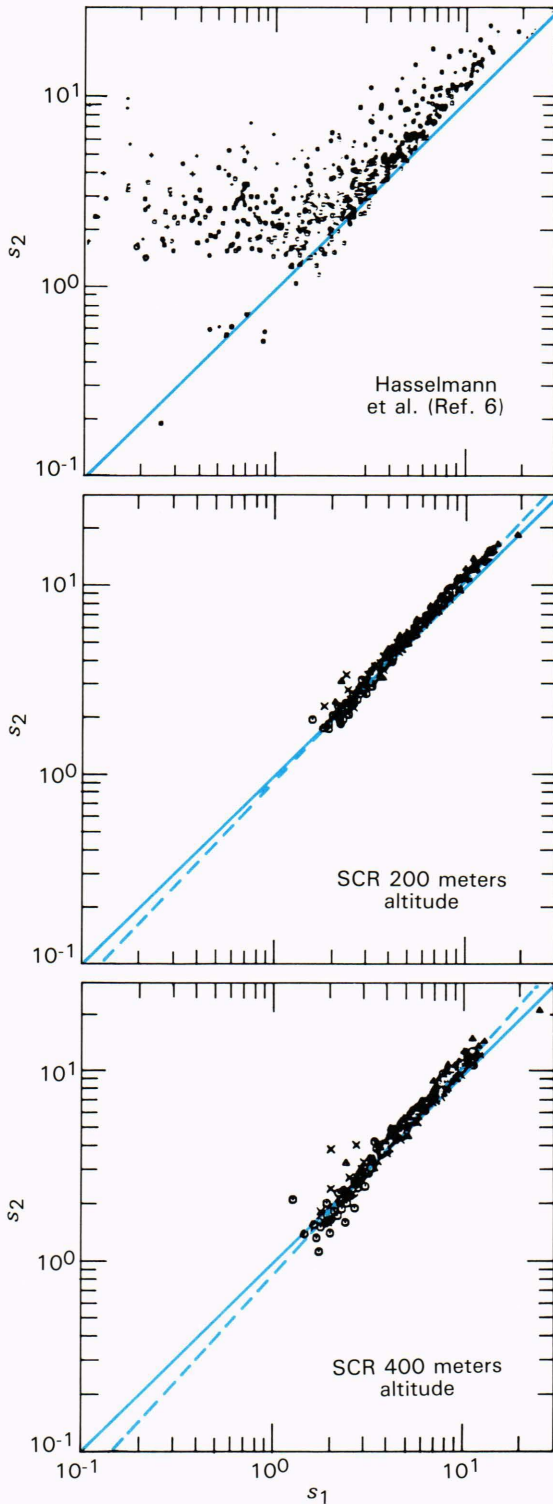


Figure 5—Comparison of the Eq. 1 spread parameter s , determined from r_1 and r_2 , for the SCR ARSLOE data sets and the values from pitch-and-roll data taken during JONSWAP

of swell to study the variation of the spreading function with wave frequency.

In analyzing the consistency of the magnitudes of the Fourier coefficients for this data set, Hasselmann et al.⁶ used a slightly different approach from that of

Cartwright.⁵ Instead of developing a scatter plot of r_2 versus r_1 , they plotted s_2 (the estimate of s in Eq. 1 obtained from r_2) versus s_1 (the estimate of s obtained from r_1). If the azimuthal energy distribution is of the form of Eq. 1, then s_1 should be identical to s_2 and all the points would fall on a line whose slope is 45 degrees. The data from Hasselmann et al.⁶ are reproduced at the top of Fig. 5. It is apparent that there is a large scatter in the data. For comparison, the SCR data points from ARSLOE have been replotted in the same format in the middle (200-meters altitude) and bottom (400 meters) of Fig. 5. Once again we see that there is virtually no scatter in the SCR data compared to the buoy data. The slope of the SCR data points appears to be slightly greater than unity, and the dotted straight lines in the figure have been least-squares fitted to the data. It is interesting that the right-side asymptote of the buoy data also has a slope that exceeds unity, but the scatter in the data was apparently so large that Hasselmann et al.⁶ did not consider it noteworthy.

HIGH SPATIAL RESOLUTION OF SURFACE CONTOUR RADAR SPECTRA

The SCR measured the directional wave spectrum in the vicinity of Delaware Bay on January 5, 1982. The wind was blowing offshore, nearly parallel to the bay axis, at approximately 20 meters per second. The left side of Fig. 6 shows a flight line flown parallel to the shoreline, starting off the New Jersey coast and ending on the axis of Delaware Bay. The heavy dots indicate the center positions of contiguous sets of 1024 scan lines (approximately 5 kilometers along track) used to produce the spectra shown on the right side of Fig. 6. The radial direction from the center of the mouth of Delaware Bay to the center of each data set was determined and indicated by the dotted radials.

The wave field defined by the SCR is thought of in terms of propagation vectors so that direction is referenced to the direction toward which the wave energy is propagating. The spectra on the right side of Fig. 6 are numbered consecutively from north to south. They show only the right half plane (0 to 180 degrees) and the wavenumber region from 0.1 to 0.3 radian per meter. Arrows show the direction from Delaware Bay, corresponding to the dotted radials on the left side of Fig. 6.

This sequence of spectra demonstrates the high spatial resolution of the SCR. Several interesting things are apparent in the sequence. In general, the spectra shift from northeast to southeast, following the radials from Delaware Bay, indicating that the waves were originating in the bay. However, the two northernmost spectra are actually propagating more northerly than the radials. Since the left side of Fig. 6 indicates that these radials graze the shoreline, part of the wave energy may have arrived in that region as the result of refraction. Refraction might also account for the energy being highest in the first spectrum and then waning over the next three.

Spectra 5 through 10 in Fig. 6 have peaks that are south of the radial from Delaware Bay, a location that

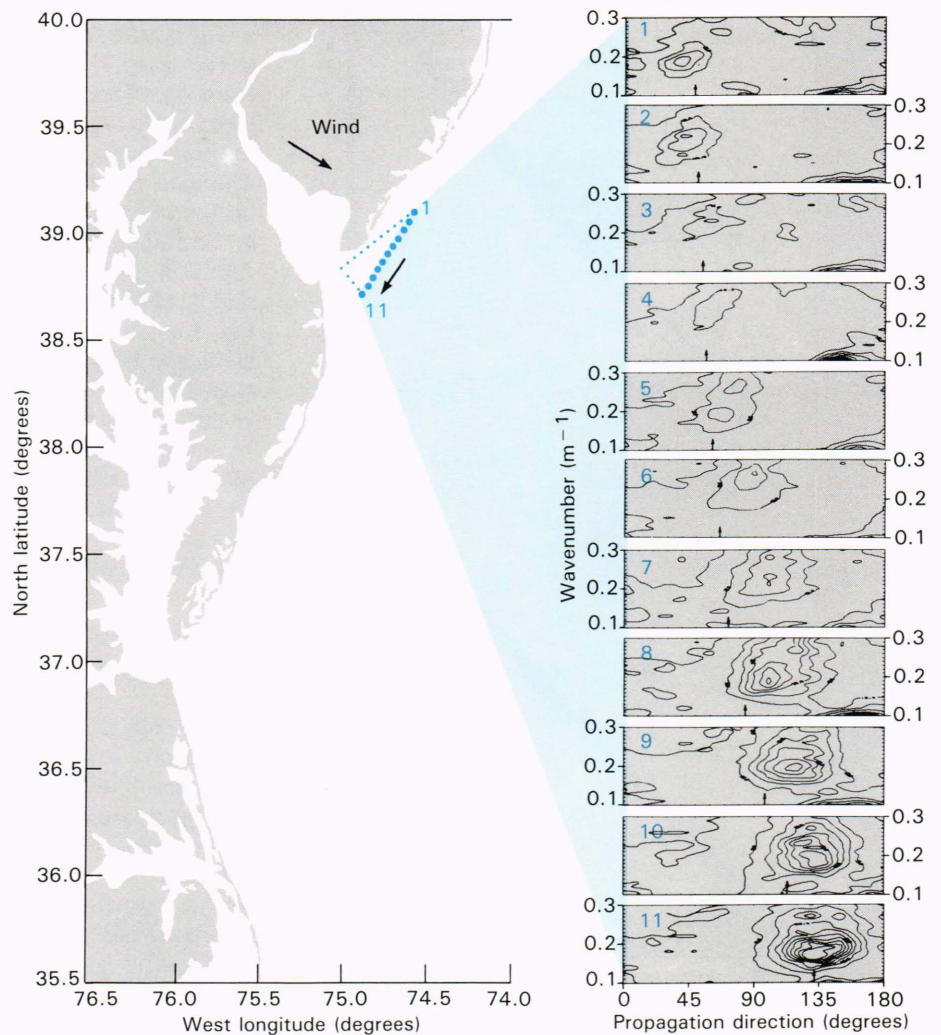


Figure 6—Shoreline in the vicinity of Delaware Bay and Chesapeake Bay. The heavy dots indicate the centers of contiguous data spans on an SCR ground track on January 5, 1982, that were used to compute the directional wave spectra shown on the right.

is reasonable since the radials were drawn from the center of the mouth of the bay, which has a significant width. The radial associated with the last spectrum, which is also the most intense, is centered on the spectral peak, and the associated radial is nearly aligned with the axis of Delaware Bay.

ELIMINATION OF PROPAGATION DIRECTION AMBIGUITY

The technique of producing directional wave spectra with the SCR has some similarities to the airborne application of stereophotography to the observation of ocean waves⁸⁻¹¹ except that the stereophotographic technique provides the instantaneous topography of the sea surface, with the result that there are no Doppler effects. An instantaneous topographic map could represent waves traveling in either of two directions, separated by 180 degrees. As was pointed out by Holthuijsen,¹¹ it is not possible to discriminate between the two spectral lobes using stereophotography, and a priori knowledge must be introduced to reject the ambiguous lobe. While that process might not be too difficult near a shoreline, it could be quite troublesome far out to sea.

Since it takes approximately 52 seconds to acquire each SCR data set used to produce a directional wave spectrum, the data do not represent an instantaneous elevation map. But far from being a disadvantage, the SCR Doppler effects are easily corrected³ and provide a means to determine uniquely the propagation direction of the waves being measured.

Figure 7 shows overlays for two different ground tracks of the Doppler-corrected directional wave spectra for the bimodal system of swell measured on October 28, 1980, off Duck, N.C., during the ARSLOE experiment. The spectral data on a $10 \text{ degree} \times 0.01 \text{ m}^{-1}$ wavenumber grid were slightly smoothed by averaging over 3×3 points with the surrounding eight points each weighted one-eighth that of the center point. The solid curves are the average of four spectra, and the colored curves are the average of two, all from data obtained at 400 meters altitude. All of the spectral components were Doppler corrected on the assumption that they were real. The corrections cause the actual spectral components (propagating toward the north and west) to coalesce for the two flight directions. But the corrections are in the wrong direction for the ambiguous lobes

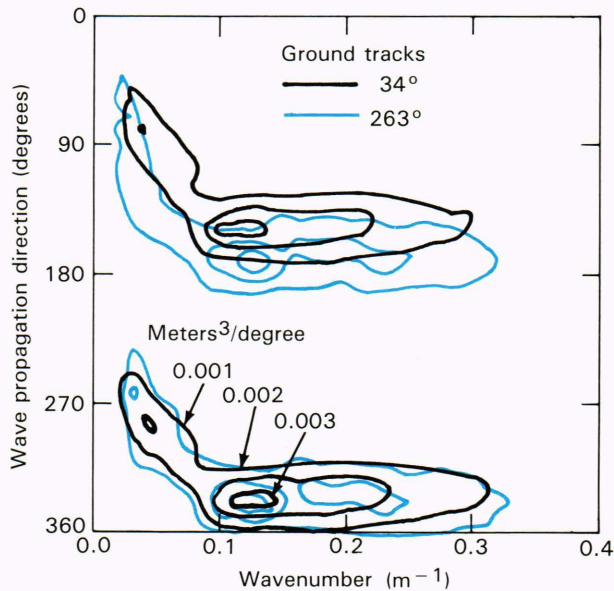


Figure 7—Overlays for two ground tracks of the Doppler-corrected directional wave spectra for a bimodal system of swell propagating toward the north and west on October 28, 1980.

(south and east) and cause the mismatch (apparent in Fig. 7) that allows them to be rejected.

ABILITY OF THE SURFACE CONTOUR RADAR TO RESOLVE COMPLEX SPECTRA

The SCR can determine even a complex spectrum in great detail. Figure 8 shows a directional wave spectrum generated from data taken at an altitude of 860 meters approximately 240 kilometers west of the eye of Hurricane Debby on September 17, 1982. The significant wave height was 4.3 meters, and the spectrum shown is the average of five spectra gathered in the 1810 to 1815 GMT interval. The aircraft was traveling at 98 meters per second along a 319-degree ground track with a drift angle of approximately -7 degrees. The SCR beam was scanning at 9.6 hertz, producing one cross-track raster scan line of elevations every time the aircraft advanced 5.1 meters.

The spectrum shows the presence of both sea and swell generated by the hurricane. By flying along different ground tracks, the ambiguous spectral lobes were rejected and are shown crossed out in the figure. The swell peak spectral density is at 0.09 hertz and has a 25-degree half-power width that Walsh et al.³ indicate is the resolution limit of the SCR at that frequency. The peak spectral density of the sea is at 0.12 hertz with a 35-degree half-power width, which is about three times as wide as the SCR resolution for those conditions.

Figure 9 shows the aircraft position relative to the hurricane ground track obtained from the forecasts. Also indicated is the expected wind at the aircraft position, derived from the hurricane forecast and confirmed by the wind measured at the aircraft altitude.

The hurricane spectrum gives an indication of the detail that the SCR can provide to those studying wave

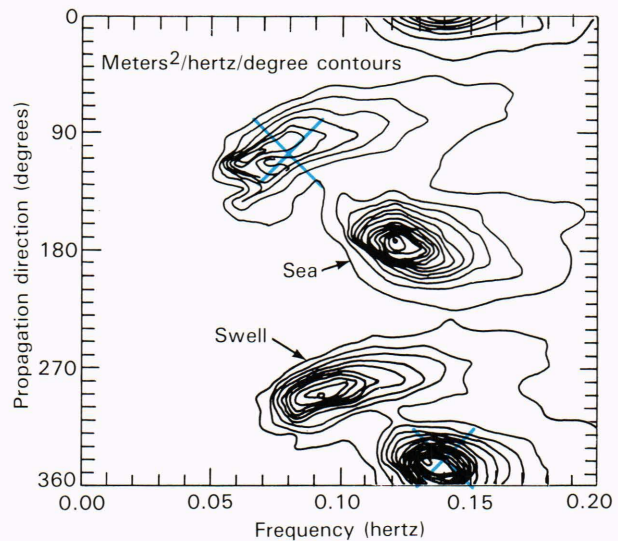


Figure 8—SCR directional wave spectrum taken in the vicinity of Hurricane Debby.

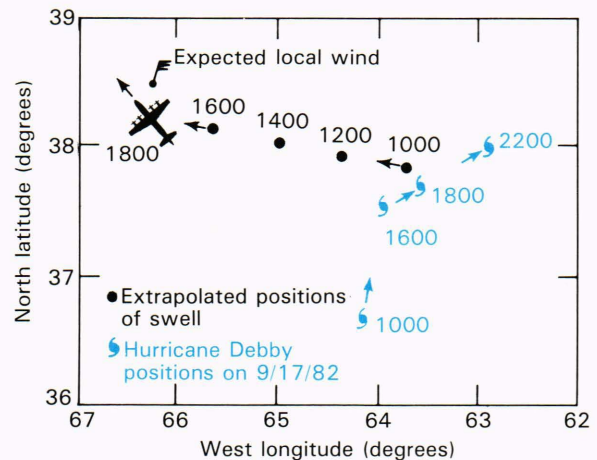


Figure 9—Plan view of the aircraft position and the Hurricane Debby ground track.

growth and dissipation under these highly nonlinear circumstances. The sea and swell spectral lobes both turn through 30 degrees in the direction of propagation as frequency increases—the sea in a clockwise direction and the swell in a counterclockwise direction. The extrapolated positions shown for the swell indicate it was generated at approximately 1000 GMT in a region 140 kilometers from the eye of the hurricane. It would have been impossible for a pitch-and-roll buoy to produce this spectral detail.

RAPID MAPPING CAPABILITY OVER EXTENSIVE AREAS

Figure 10 shows two ground tracks flown in the downwind direction during fetch-limited conditions in January: one in 1982 when the wind was approximately 20 meters per second and one in 1983 when it was approx-

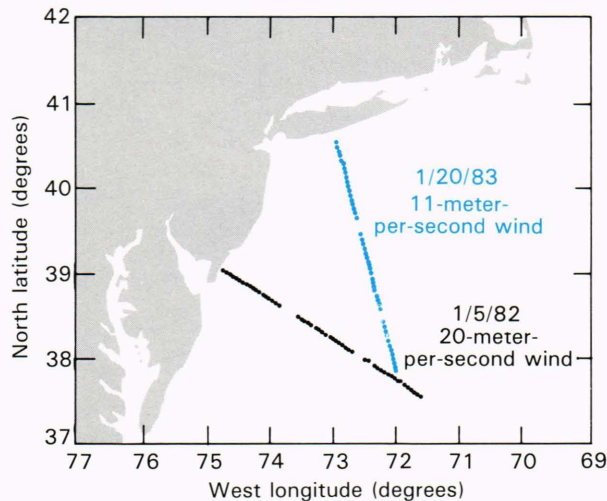


Figure 10—Two ground tracks flown in the downwind direction during fetch-limited conditions.

imately 11 meters per second. Figure 11 shows three curves that indicate the growth of the significant wave height with fetch predicted by the JONSWAP empirical relationship¹² for wind speeds of 10, 15, and 20 meters per second. Also shown is the significant wave-height variation measured by the SCR on the two ground tracks indicated in Fig. 10. The wave height is somewhat higher than predicted for the 20-meter-per-second wind on January 5, 1982, because the wave growth got a head start in Delaware Bay, which was nearly aligned with the wind direction. The significant wave height was also duration-limited to 5 meters because the wind had been blowing for only 14 hours.

Figure 12 shows the entire set of 48 SCR wave spectra obtained within an hour on the downwind leg on January 20, 1983, as 16 nonoverlapping averages of three spectra. The contours indicate the 0.1, 0.3, 0.5, 0.7, and 0.9 levels relative to the peak. In this sequence the spectrum evolves quickly at first in shape, wavenumber, and propagation direction, but after the eleventh or twelfth average spectrum, there is little change and no trend.

Although the wind had been blowing in the approximate direction of the aircraft ground track for more than a day prior to the flight on January 20, 1983, it had shifted and was blowing from approximately 5 degrees for 3 hours before the start of the run. The recent wind was responsible for the wave propagation direction near shore, but as the aircraft proceeded offshore, it was essentially looking back in time, because greater fetches require longer integration times and the wave field veered into what had been the prevailing downwind direction.

SUMMARY

The SCR and the AOL can provide a direct measurement of the topography of ocean waves from an operating altitude of 200 to 800 meters. The profiling AOL

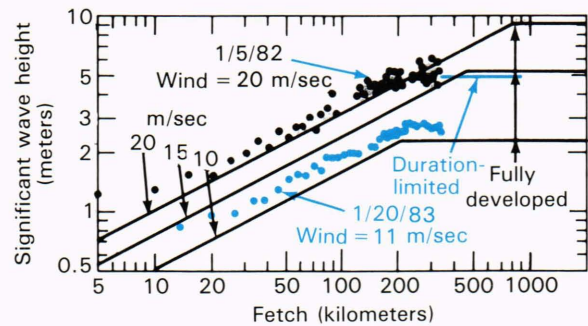


Figure 11—Three curves indicating the growth of the significant wave height with fetch predicted by the JONSWAP empirical relationship and the significant wave height variation measured by the SCR on the two ground tracks indicated in Fig. 10.

can provide a spectrum that is close to the nondirectional ocean-wave spectrum for ground tracks that are parallel to the direction of propagation of the waves. The SCR can provide the full directional wave spectrum with high spatial resolution (5 kilometers) and with better azimuthal resolution than pitch-and-roll buoys. It can also eliminate the propagation-direction ambiguity that is present in a number of other wave-measurement techniques.

REFERENCES

- 1 J. E. Kenney, E. A. Uliana, and E. J. Walsh, "The Surface Contour Radar, a Unique Remote Sensing Instrument," *IEEE Trans. Microwave Theory Tech.* **MTT 27**, 1080-1092 (1979).
- 2 F. E. Hoge, R. N. Swift, and E. B. Frederick, "Water Depth Measurement Using an Airborne Pulsed Neon Laser System," *Appl. Opt.* **19**, 871-887 (1980).
- 3 E. J. Walsh, D. W. Hancock, D. E. Hines, R. N. Swift, and J. F. Scott, "Directional Wave Spectra Measured with the Surface Contour Radar," *J. Phys. Oceanogr.* **15**, 566-592 (1985).
- 4 M. S. Longuet-Higgins, D. E. Cartwright, and N. D. Smith, "Observations of the Directional Spectrum of Sea Waves Using the Motions of a Floating Buoy," in *Ocean Wave Spectra*, Prentice-Hall, pp. 111-136 (1963).
- 5 D. E. Cartwright, "The Use of Directional Spectra in Studying the Output of a Wave Recorder on a Moving Ship," in *Ocean Wave Spectra*, Prentice-Hall, pp. 203-218 (1963).
- 6 D. E. Hasselmann, M. Duncel, and J. A. Ewing, "Directional Wave Spectra Observed During JONSWAP 1973," *J. Phys. Oceanogr.* **10**, 1264-1280 (1980).
- 7 L. Baer and C. L. Vincent, eds., Special Issue on Atlantic Remote Sensing Land Ocean Experiment (ARSLOE), *IEEE J. Oceanic Eng.* **OE-8**, 201-271 (1983).
- 8 L. J. Coté, J. O. Davis, W. Marks, R. J. McGough, E. Mehr, W. J. Pierson, J. F. Ropek, G. Stephenson, and R. C. Vetter, "The Directional Spectrum of a Wind Generated Sea as Determined from Data Obtained by the Stereo Wave Observation Project," *Meteorol. Papers 2*, College of Engineering, New York University (1960).
- 9 L. S. Simpson, "Preliminary Investigation of the Directional Spectrum of Ocean Wave Height as Obtained from Stereo Wave Photographs," *Informal Manuscript No. 67.1*, U.S. Naval Oceanographic Office, Washington, D.C. (1967).
- 10 Y. Sugimori, "A Study of the Application of the Holographic Method to the Determination of the Directional Spectrum of Ocean Waves," *Deep-Sea Res.* **22**, 339-350 (1975).
- 11 L. H. Holthuijsen, "Observations of the Directional Distribution of Ocean-Wave Energy in Fetch-Limited Conditions," *J. Phys. Oceanogr.* **13**, 191-207 (1983).
- 12 K. Hasselmann, T. P. Barnett, E. Bouws, H. Carlson, D. E. Cartwright, K. Enke, J. A. Ewing, H. Gienapp, D. E. Hasselmann, P. Kruseman, A. Meerburg, P. Muller, D. J. Olbers, K. Richter, W. Sell, and H. Walden, "Measurements of Wind-Wave Growth and Swell Decay During the Joint North Sea Wave Project (JONSWAP)," *Deut. Hydrog. Z., Suppl. A.* **8** (1973).

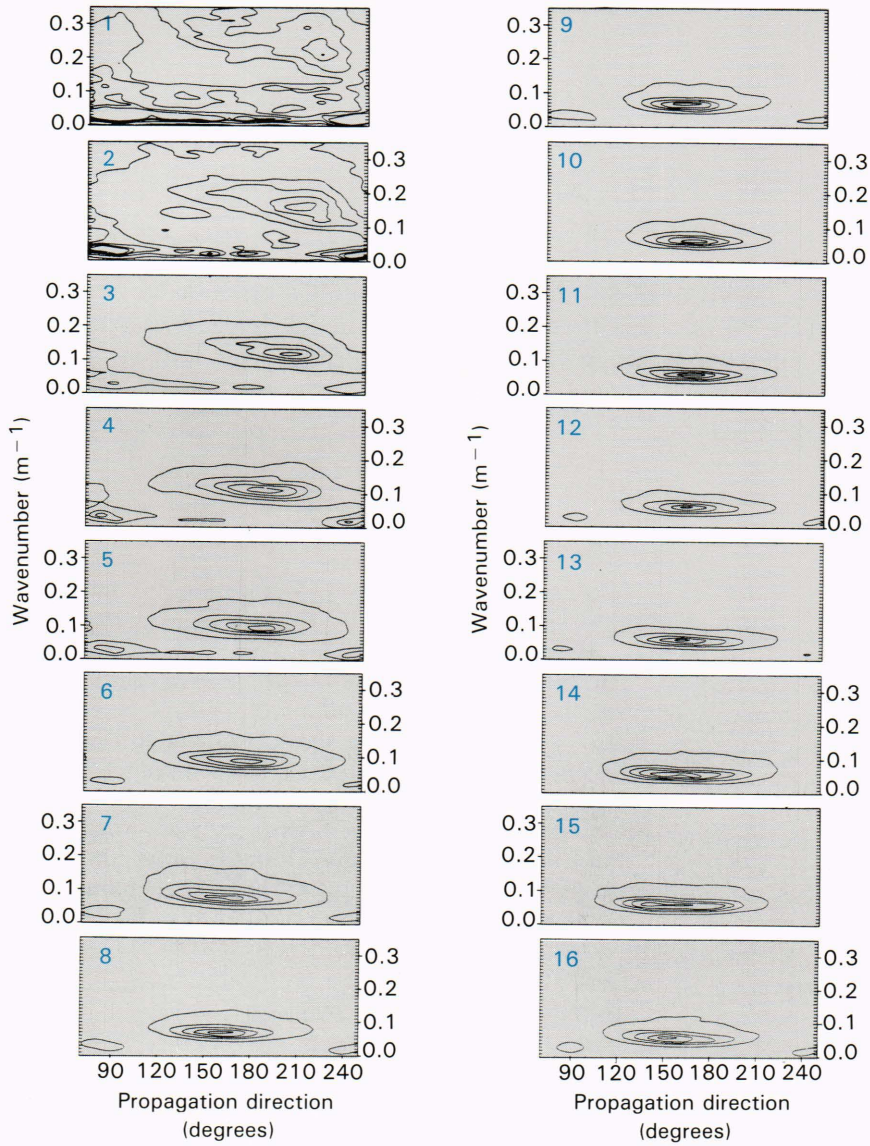


Figure 12—Sixteen nonoverlapping three-spectra averages of the 48 SCR wave spectra obtained on the downwind leg on January 20, 1983.